New Thiostannates Synthesized Under Solvothermal Conditions: Crystal Structures of (trenH)$_2$Sn$_3$S$_7$ and {[Mn(tren)]$_2$Sn$_2$S$_6$}

Nicole Pienack, Diana Schinkel, Angela Puls, Marie-Eve Ordolff, Henning Lühmann, Christian Näther, and Wolfgang Bensch

Institute of Inorganic Chemistry, Christian-Albrechts University of Kiel, Max-Eyth-Str. 2, 24118 Kiel, Germany

Reprint requests to Prof. W. Bensch. Phone: +49 431 880-2419. Fax: +49 431 880-1520.
E-mail: wbensch@ac.uni-kiel.de

Dedicated to Professor Heribert Offermanns on the occasion of his 75th birthday

The two new thiostannate compounds (trenH)$_2$Sn$_3$S$_7$ (**1**) and {[Mn(tren)]$_2$Sn$_2$S$_6$} (**2**) (tren = tris-2-aminoethylamine) were obtained under solvothermal conditions. Compound **1** crystallizes in the hexagonal space group $P6_3/mmc$ with $a = 13.2642(19)$, $c = 19.078(3)$ Å, $V = 2906.9(7)$ Å^3. The layered [Sn$_3$S$_7$]$^{2-}$ anion is constructed by Sn$_3$S$_4$ semi-cubes sharing common edges. The layers are characterized by large hexagonal pores with dimensions of about 11×11 Å^2. Compound **2** crystallizes in the triclinic space group $P\bar{1}$ with lattice parameters $a = 7.6485(7)$, $b = 8.1062(7)$, $c = 12.1805(11)$ Å, $\alpha = 97.367(11)$, $\beta = 103.995(11)$, $\gamma = 108.762(10)°$, $V = 676.17(10)$ Å^3. The [Sn$_2$S$_6$]$^{4-}$ anion is composed of two edge-sharing SnS$_4$ tetrahedra and joins two Mn^{2+}-centered complexes by Mn–S bond formation. The Mn^{2+} cation is in a trigonal-bipyramidal environment of four N atoms of the tren ligand and one S atom of the thiostannate anion. Both compounds are semiconductors with a band gap of 2.96 eV for **1** and of 2.75 eV for **2**.

Key words: Thiostannates, Solvothermal Syntheses, Crystal Structure

Introduction

In the last decades a large number of thiometalate compounds were prepared following the solvothermal approach, and the fascinating chemistry of these compounds was discussed in several review articles [1 – 5]. Among the thiometalates, thiostannates are an attractive group of compounds exhibiting promising, zeolite-like properties and interesting structural features [1 – 8]. The negative charge of the anionic thiostannate networks can be compensated in three different ways: 1. metal cations are integrated in the network yielding pure inorganic compounds, 2. organic molecules, protonated amine molecules or transition metal complexes (*TMC*) serve as counterions, and 3. *TMC*s are part of the networks with bond formation between the thiostannate and the *TMC*. The first thiostannates with organic or protonated amine molecules acting as charge-compensating cations were synthesized under solvothermal conditions applying alkyl ammonium cations. Bedard introduced the no-

tation "*R-M'MS-n*" for the new thiostannates [9 – 11]. The structure-directing agents *R* act also as charge-compensating cations, *M'* represents a 3*d* or 4*d* metal cation and *M* the network atom (Ge, Sn, Sb, In). The number *n* distinguishes between different structure types. The solvothermal syntheses were conducted with metal sulfides, or metals and sulfur, and the corresponding amine solutions or alkyl ammonium salts. In most cases lamellar structures were formed. The common structure types *R*-SnS-1 and *R*-SnS-3 are built of two-dimensional layers ([Sn$_3$S$_7$]$^{2-}$ resp. [Sn$_4$S$_9$]$^{2-}$) with Sn$_3$S$_4$ semi-cubes as main structural motifs. These well-known thiostannate families feature many members, and several interesting experiments were done with outstanding results [12]. In the meantime, a relatively large number of thiostannates have been synthesized under solvothermal conditions applying different structure-directing agents [13 – 19]. The main goal of many experiments designed to obtain a thiostannate material that combines the properties of zeolites with the optical and electronic properties of

semiconductors could not be reached due to the fact that the structure-directing molecules located in and/or below pores, in channels or between layers, cannot be removed without a collapse of the inorganic network. Nevertheless, due to their rich structural features and semiconducting properties, thiostannates are possible candidates for various applications including chemical sensing [20 – 23].

Alterations of the physico-chemical properties of thiostannates can be achieved by integrating transition metal complexes (*TMC*) into the networks, and the potential of this approach is impressively demonstrated by many examples (see for example ref. [12]). In the overwhelming number of examples the thiostannates contain TM^{n+} complexes and discrete thiostannate anions. In most structures the dimeric ion [Sn$_2$S$_6$]$^{4-}$ is found like in [Ni(en)$_3$]$_2$Sn$_2$S$_6$ [24, 25], [Ni(dien)$_2$]$_2$Sn$_2$S$_6$ [24], [Co(en)$_3$]$_2$Sn$_2$S$_6$, [Zn(en)$_3$]$_2$ Sn$_2$S$_6$, [Mn(en)$_2$]$_2$Sn$_2$S$_6$ [26], [Mn(en)$_3$]$_2$Sn$_2$S$_6$ ·2 H$_2$O, and [Mn(dien)$_2$]$_2$Sn$_2$S$_6$ [27] (en = ethylene-diamine, dien = diethylenetriamine). One should keep in mind that *e. g.* Ni^{2+} or Co^{2+} favor bond formation to nitrogen instead of sulfur and therefore the bonding to the thiostannate network is often prevented. With the chalcophilic elements Cu or Ag the integration is easily achieved and examples are (DBUH)CuSnS$_3$, (1,4-dabH$_2$)Cu$_2$SnS$_4$ [28], (DBNH)$_2$Cu$_2$Sn$_2$S$_8$ [29], (H$_2$en)$_2$Cu$_8$Sn$_3$S$_{12}$ [30], (enH)$_{6+n}$Cu$_{40}$Sn$_{15}$S$_{60}$, (enH)$_3$Cu$_7$Sn$_4$S$_{12}$ [31], (NH$_4$)$_2$Ag$_6$Sn$_3$S$_{10}$ [32], and (1,4-dabH$_2$)Ag$_2$SnS$_4$ [33] (DBU = 1,8-diaza-bicyclo[5.4.0]undec-7-ene, 1,4-dab = 1,4-diaminobu-tane, DBN = 1,5-diazabicyclo[4.3.0]non-5-ene). During our studies the usage of Mn^{2+} proved to be successful to connect [Mn(amine)$_x$]$^{y+}$ complexes to the thiostannate network, and some interesting compounds like (1,4-dabH)$_2$MnSnS$_4$ [34], [{Mn(1,2-dach)$_2$(H$_2$O)}$_2$Sn$_2$S$_6$], [{Mn(1,2-dach)$_2$} Sn$_2$S$_6$] · 2 (1,2-dach) [35] and [{Mn(trien)}$_2$SnS$_4$]·4 H$_2$O [36] with novel structural features were obtained (1,2-dach = 1,2-diaminocyclohexane, trien = triethylenetetramine). Further examples like [{Mn(en)$_2$}$_2$(μ-en)(μ-Sn$_2$S$_6$)]$_x$ [37], {[Mn(en)$_2$]$_2$ Sn$_2$S$_6$} [38] or {[Mn(phen)]$_2$SnS$_4$}$_n$· n H$_2$O (phen = 1,10-phenanthroline) [39] feature interesting structures were also prepared under solvothermal conditions.

In this paper we present the two new thiostann-ates (trenH)$_2$Sn$_3$S$_7$ (**1**) and {[Mn(tren)]$_2$Sn$_2$S$_6$} (**2**) (tren = tris-2-aminoethylamine) exhibiting inter-esting characteristics. The second compound was obtained during the experiments to integrate Mn^{2+} into [Sn$_3$S$_7$]$^{2-}$ layers.

Experimental Section

Synthesis

General: All chemicals were purchased (see below for purity and source) and used without further purifications. All compounds were prepared under solvothermal conditions in Teflon-lined steel autoclaves (inner volume 30 mL) or glass tubes (inner volume 7 mL) using tin, manganese, sulfur and amine. The crystalline products were filtered off after the reactions, washed with water and ethanol or acetone and dried in a vacuum. The reaction products were separated manually, and the homogeneity was checked by powder X-ray diffraction and elemental analysis.

Synthesis of (trenH)$_2$Sn$_3$S$_7$ (**1**)

249.0 mg (2.1 mmol) of tin (99.5 %, Aldrich) and 150.4 mg (4.7 mmol) of sulfur were heated in 4 mL of tris-2-aminoethylamine (C$_6$H$_{18}$N$_4$, tren) ($\geq$ 96 %, Acros Organics) for ten days at 200 °C. In the reaction products, yellow hexagonal-shaped plates were obtained in a yield of 15 % (based on Sn). Shorter reaction times lead to products with poor crystal quality. Elemental analysis (%): calcd. C 16.5, H 4.4, N 12.8; found C 16.3, H 4.4, N 13.4.

Synthesis of {[Mn(tren)]$_2$Sn$_2$S$_6$} (**2**)

54.9 mg (1 mmol) of manganese, 118.7 mg (1 mmol) of tin and 96.2 mg (3 mmol) of sulfur were reacted with 2 mL of a 50 % aqueous solution of tren using a diffusion cell. The mixture was heated at 180 °C for 7 days. The yield of the light-yellow needles was about 15 % – 20 % (based on Sn). Elemental analysis (%): calcd. C 17.3, H 4.4, N 13.5; found C 17.3, H 4.5, N 13.2.

Structure determinations

The intensity data were collected using a Stoe IPDS-1 with MoK_α (λ = 0.71073 Å) radiation at room temperature. The structures were solved with Direct Methods using the program SHELXS-97 [40], and the refinements were carried out against F^2 with SHELXL-97 [41]. All non-hydrogen atoms were refined with anisotropic displacement parameters. The amine molecules in **1** are strongly disordered and could not be localized during the structure refinement. Therefore, the data were corrected for disordered solvent using the SQEEZE option in PLATON [42]. Calculation of the volume available for solvent molecules with PLATON yields 1975.8 Å^3 which is large enough to host two molecules of tris-2-aminoethylamine.

	(trenH)$_2$Sn$_3$S$_7$ (**1**)	{[Mn(tren)]$_2$Sn$_2$S$_6$} (**2**)
Crystal system	hexagonal	triclinic
Space group	$P6_3/mmc$	$P\bar{1}$
a, Å	13.2642(19)	7.6485(7)
b, Å	13.2642(19)	8.1062(7)
c, Å	19.078(3)	12.1805(11)
α, deg	90	97.367(11)
β, deg	90	103.995(11)
γ, deg	120	108.762(10)
V, Å^3	2906.9(7)	676.17(10)
Z	4	1
D_{calcd}, g cm^{-3}	1.33	2.03
μ(MoK_α), mm^{-1}	3.0	3.2
Scan range, deg	$1.77 \leq \theta \leq 27.03$	$2.72 \leq \theta \leq 25.92$
Reflections collected	6383	4676
Independent reflections	1240	2046
Refl. with $F_o > 4\,\sigma(F_o)$	1048	410
Final $R1$ / $wR2$ [$I > 2\,\sigma(I)$]	0.0442 / 0.1122	0.0332 / 0.0704
Final $R1$ / $wR2$ (all data)	0.0588 / 0.1149	0.0513 / 0.0746
Goodness-of-fit on F^2	1.060	0.953
$\Delta\rho_{fin}$ (max / min), e Å^{-3}	0.93 / −0.63	1.26 / −0.79

Table 1. Crystal data and selected details of the data collection and structure refinement results.

For compound **2** all non-hydrogen atoms were refined with anisotropic displacement parameters. The hydrogen atoms were positioned with idealized geometry and were refined using a riding model. The crystal was non-merohedrically twinned, and the reflections of both individuals were indexed separately, and the intensities were integrated using the TWIN option in the IPDS-1 program package. Overlapping reflections were omitted. Therefore, the completeness is only 77.7 %. Selected structural data and refinement results are summarized in Table 1.

CCDC 887622 (**1**) and CCDC 887623 (**2**) contain the supplementary crystallographic data for this paper. These data can be obtained free of charge from The Cambridge Crystallographic Data Centre *via* www.ccdc.cam.ac.uk/data_request/cif.

SEM-EDX analysis

Scanning electron microscopy investigations (SEM) and energy dispersive X-ray analyses (EDX) were performed with a Philips Environmental Scanning Electron Microscope ESEM XL30 equipped with an EDAX detector.

Powder X-ray diffractometry

The powder X-ray diffraction patterns were recorded on a Stoe Stadi-P powder diffractometer (Cu$K_{\alpha1}$ radiation, $\lambda = 1.540598$ Å, Ge monochromator) in transmission geometry.

Thermal investigations

The thermal measurements were performed on a Netzsch STA 429 DTA-TG measurement device. The samples were heated to 500 °C with a rate of 4 K·min^{-1} under a flow of argon (75 mL·min^{-1}) in Al$_2$O$_3$ crucibles. The TG data were corrected for buoyancy and current effects. The experiments have shown that **1** starts to decompose at about 230 °C ($T_{onset} = 237$ °C), while **2** is stable up to 320 °C ($T_{onset} = 329$ °C).

Infrared spectroscopy

MIR spectra ($500 - 4000$ cm^{-1}) were recorded with an ATI Mattson Genesis spectrometer. For compound **1** the absorptions located at 3308 (s, -NH$_2$ stretch), 3246 (m, -NH$_2$ stretch, -NH$_3^+$), 2917 (m, -NH$_2$ stretch, -NH$_3^+$), 2814 (m, -CH stretch, N-CH$_2$), 1630 (m, -C-N-H def.), 1565 (s, -NH$_2$ asym. def.), 1468 and 1453 (s, -CH def., N-CH$_2$), 1388 and 1366 (s, -CH def.), 1120 (s, -CN stretch), 1097 (s, -CN stretch), 1071 (s, -CN stretch) and 1051 (s, -CN stretch) cm^{-1} can be assigned to the tris-2-aminoethylamine. For compound **2** absorptions at 3308 (s, -NH$_2$ stretch), 3264 (m, -NH$_2$ stretch), 3094 (m, -NH$_2$ stretch), 2862 (m, -CH stretch, N-CH$_2$), 1576 (s, -NH$_2$ asym. def.), 1448 (s, -CH def., N-CH$_2$), 1349 and 1304 (s, -CH def.), 1083 (s, -CN stretch) and 1024 (s, -CN stretch) cm^{-1} are observed.

Raman spectroscopy

Raman spectra were recorded with a Bruker IFS 66 Fourier transform Raman spectrometer (wavelength: 541.5 nm) in the range from 100 to 3500 cm^{-1}.

UV/Vis spectroscopy

UV/Vis spectroscopic investigations were carried out at room temperature using an UV/Vis/NIR two-channel spectrometer Cary 5 from Varian Techtron Pty., Darmstadt. The optical properties of the thiostannates were investigated by

Sn(1)–S(3)	2.390(2)	S(3)–Sn(1)–S(2)	123.24(6)	Table 2. Selected Sn–S bond lengths (Å) and S–Sn–S angles (deg) in the structure of **1**^{a}.
Sn(1)–S(2)	2.4364(13)	S(2)–Sn(1)–S(2)a	113.34(11)	
Sn(1)–S(2)a	2.4364(13)	S(3)–Sn(1)–S(3)b	89.05(7)	
Sn(1)–S(3)b	2.5353(19)	S(2)–Sn(1)–S(3)b	92.70(5)	
Sn(1)–S(1)	2.6074(19)	S(3)–Sn(1)–S(1)	91.45(7)	
S(1)–Sn(1)c	2.6074(19)	S(2)–Sn(1)–S(1)	87.02(5)	
S(1)–Sn(1)a	2.6074(19)	S(3)b–Sn(1)–S(1)	179.50(7)	
S(2)–Sn(1)c	2.4364(13)	Sn(1)–S(1)–Sn(1)a	87.39(8)	
S(3)–Sn(1)b	2.5352(19)	Sn(1)–S(2)–Sn(1)c	95.35(7)	
		Sn(1)–S(3)–Sn(1)b	90.95(7)	

^{a} Symmetry transformations used to generate equivalent atoms: a: $-x+y+1$, $-x+1$, z; b: $-x+1$, $-y$, $-z+1$; c: $-y+1$, $x-y$, z

analyzing the UV/Vis reflectance spectra of the powdered samples (with BaSO$_4$ powder used as reference material). The absorption data were calculated applying the Kubelka-Munk relation for diffuse reflectance data. The optical band gap of **1** was estimated to 2.96 eV, and for **2** the band gap is about 2.75 eV.

Results and Discussion

Crystal structure of (trenH)$_2$Sn$_3$S$_7$ (**1**)

The compound crystallizes in the hexagonal space group $P6_3/mmc$ with 4 formula units in the unit cell. The layered [Sn$_3$S$_7$]$^{2-}$ anion contains Sn$_3$S$_4$ semi-cubes which are formed *via* edge-sharing of SnS$_5$ trigonal bipyramids (Fig. 1).

The Sn–S bonds are in the range from 2.390(2) to 2.6074(2) Å with S–Sn–S angles varying between 87.02(5) and 179.50(7)° (Table 3).
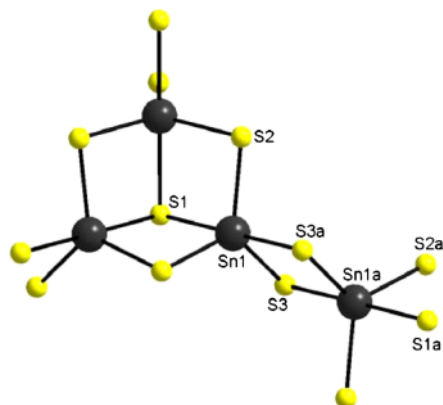
All values are in good agreement with the literature data [16, 18, 19]. The Sn$_3$S$_4$ semi-cubes are joined *via* two S^{2-} anions yielding anionic layers with hexagonal-shaped 24-atom rings (Fig. 2).

The dimension of the pores is about 10.9×10.9 Å^2. Perpendicular to [001] the layers are stacked in a way that channels are generated along the same direction. The interlayer distance is about 6.04 Å. The amine molecules act as charge compensating cations, but could not be located during structure solution and refinement due to severe structural disorder. Nevertheless, on the basis of the structure of similar compounds it can be assumed that the cations are located below/above the pores. The void space of 1975.8 Å^3 as calculated with PLATON is about 67% of the unit cell volume. Comparable void spaces are
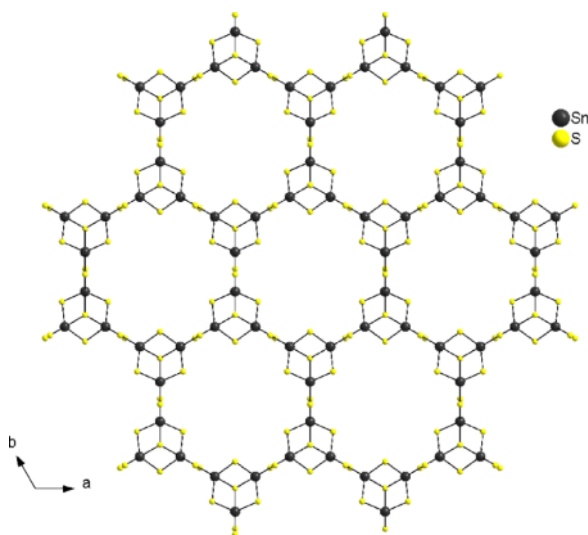

Fig. 1 (color online). The Sn$_3$S$_4$ semi-cube and the edge-sharing connection by a SnS$_5$ trigonal bipyramid generating an Sn$_2$S$_2$ ring. The atoms generated by symmetry are labelled with a (see also Table 2).

Fig. 2 (color online). The [Sn$_3$S$_7$]$^{2-}$ anionic layer (view along [001]) with hexagonal-shaped pores in the structure of **1**.

Sn(1)–S(2)	2.3155(14)	S(2)–Sn(1)–S(1)	113.00(6)	**Table 3.** Selected bond lengths (Å) and angles (deg) in the structure of **2**[a].
Sn(1)–S(1)	2.3618(13)	S(2)–Sn(1)–S(3)a	112.28(5)	
Sn(1)–S(3)a	2.4583(17)	S(1)–Sn(1)–S(3)a	113.60(5)	
Sn(1)–S(3)	2.4677(15)	S(2)–Sn(1)–S(3)	113.60(5)	
Mn(1)–N(1)	2.234(5)	S(1)–Sn(1)–S(3)	110.03(5)	
Mn(1)–N(3)	2.243(5)	S(3)a–Sn(1)–S(3)	92.77(5)	
Mn(1)–N(4)	2.267(6)	N(1)–Mn(1)–N(3)	141.32(19)	
Mn(1)–N(2)	2.346(5)	N(1)–Mn(1)–N(4)	104.1(2)	
Mn(1)–S(1)	2.4931(16)	N(3)–Mn(1)–N(4)	93.41(19)	
S(3)–Sn(1)a	2.4583(16)	N(1)–Mn(1)–N(2)	75.99(18)	
		N(3)–Mn(1)–N(2)	75.25(18)	
Sn(1)–S(1)–Mn(1)	110.02(6)	N(4)–Mn(1)–N(2)	76.03(18)	
Sn(1)a–S(3)–Sn(1)	87.23(5)	N(1)–Mn(1)–S(1)	107.59(13)	
N(2)–Mn(1)–S(1)	171.13(13)	N(3)–Mn(1)–S(1)	104.76(15)	
N(4)–Mn(1)–S(1)	95.15(13)			

[a] Symmetry transformation used to generate equivalent atoms: a: $-x+1, -y+2, -z+1$.

obtained for similar compounds *e. g.* 1614.9 Å^3 ($\approx 63\%$) for (Me$_4$N)$_2$Sn$_3$S$_7$ [16], 1785.2 Å^3 ($\approx 66\%$) for (Et$_4$N)$_2$Sn$_3$S$_7$ [19] and 3028.9 Å^3 ($\approx 62\%$) for (DABCOH)$_2$Sn$_3$S$_7$ (DABCO = 1,4-diazabicyclo[2.2.2]octane) [18].

The SEM image of a crystal of **1** (Fig. 3, left) shows the layered nature of the material with thin platelets stacked onto each other. An image taken with a light microscope is presented in Fig. 3, right, demonstrating the (pseudo)-hexagonal shape.

Compound **1** is a new member of the thiostannate family *R*-SnS-1 [43, 44]. In *R*-SnS-1, the two-dimensional [Sn$_3$S$_7$]$^{2-}$ anionic layers exhibit rings consisting of 24 atoms with pore dimensions from 10 to 11 Å, depending on the size of the charge-compensating cations/amines *R*. The organic molecules are located above/below the pores and between the layers [45]. Typical values of the interlayer distances are about 7 to 9 Å depending on the size and orientation of *R* located in the interlayer galleries [46]. In the literature, there are also some examples where the organic structure-directing molecules were replaced by alkali metal ions, *e. g.* in the thiostannates Rb$_2$Sn$_3$S$_7 \cdot$2 H$_2$O or Cs$_4$Sn$_5$S$_{12} \cdot$2 H$_2$O [47] which also contain Sn$_3$S$_4$ groups as well as Sn$_2$S$_2$ rings. In Rb$_2$Sn$_3$S$_7 \cdot$2 H$_2$O the anionic layers are constructed by face-sharing semi-cubes and bridging Sn$_2$S$_2$ rings, and in Cs$_4$Sn$_5$S$_{12} \cdot$2 H$_2$O two Sn$_3$S$_4$ semi-cubes are linked by two bridging S^{2-} anions to form the anionic layers containing elliptical pores with a diameter of about 7.3×9.9 Å^2.

Crystal structure of {[Mn(tren)]$_2$Sn$_2$S$_6$} (2)

Compound **2** crystallizes in the triclinic space group $P\bar{1}$ with one formula unit in the unit cell. The structure is composed of the bitedrahedral [Sn$_2$S$_6$]$^{4-}$ anion composed of two edge-sharing SnS$_4$ tetrahedra. Two [Mn(tren)]$^{2+}$ cations are connected to the [Sn$_2$S$_6$]$^{4-}$ unit *via* bond formation between Mn^{2+} and the S atoms S1 and S1a (see Fig. 4).

The Mn^{2+} cation is trigonal-bipyramidally coordinated by the four N atoms of the ligand and one S atom of the thiostannate anion. The N–Mn–N an-
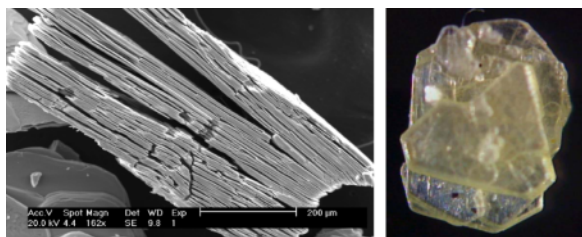

Fig. 3 (color online). SEM image (left) and a light microscope picture (right) of light-yellow plates of (trenH)$_2$Sn$_3$S$_7$ (**1**).
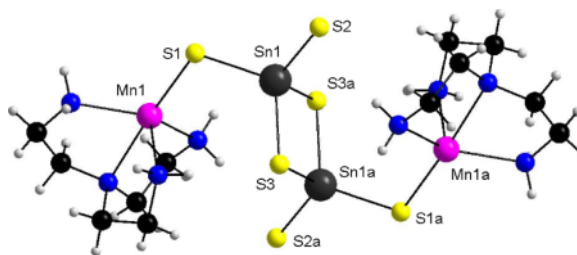

Fig. 4 (color online). Structure of {[Mn(tren)]$_2$Sn$_2$S$_6$}. The atoms generated by symmetry are labelled with a (see also Table 3).
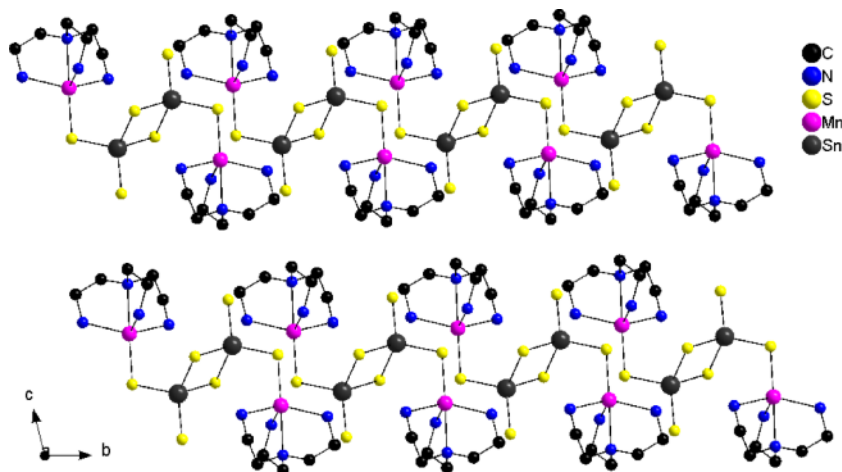
Fig. 5 (color online). Packing of the {[Mn(tren)]$_2$Sn$_2$S$_6$} molecules in the structure of **2**. The hydrogen atoms are omitted for clarity.
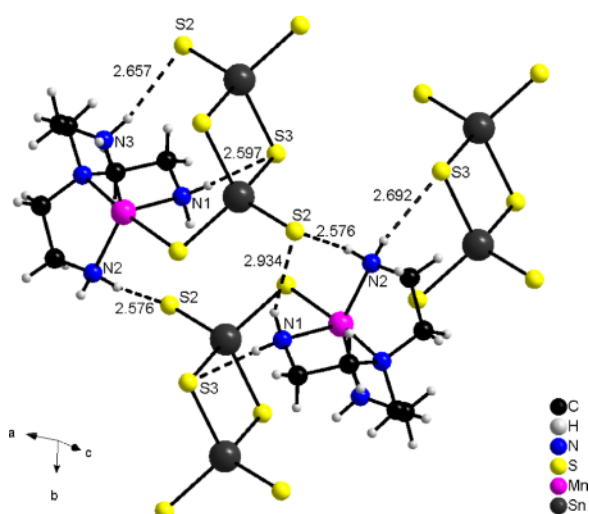

Fig. 6 (color online). Hydrogen bonding pattern in compound **2** with distances in Å.

gles (Table 3) with values ranging from 93.41(19) to 141.32(19)° indicate a pronounced distortion of the trigonal bipyramid. The N(2)–Mn(1)–S(1) angle of 171.13(13)° also differs significantly from the ideal value. The Mn–N bond lengths (2.234(5) – 2.346(5) Å) and the Mn–S bond (2.4931(16) Å) are in the range reported for [Mn(amine)]$^{2+}$ complexes integrated in thiometalates [48 – 54]. The longest Mn–N bond is in *trans*-position to the Mn–S bond. Some compounds were reported in the literature featuring also a MnN$_4$S trigonal bipyramid, like *e. g.* in the thioantimonates [Mn(tren)]Sb$_4$S$_7$ [52], [Mn(trien)]Sb$_4$S$_7$ [55],

and the thioarsenates {[Mn(tren)](As$_4$S$_7$)} [56] or [Mn(tren)]$_4$(In$_2$As$_2$S$_8$)$_2$ [57].

Both bridging Sn–S bonds (Sn–S3 and Sn–S3a) are significantly longer with 2.4677(15) and 2.4583(17) Å than the Sn–S bonds to the terminal S atoms with 2.3618(13) and 2.3155(14) Å. This behavior of the bond length distribution in the [Sn$_2$S$_6$]$^{4-}$ anion is well documented in the literature [13, 25, 58]. The angle around the Sn atom (S3–Sn1–Sn3a) in the planar Sn$_2$S$_2$ ring of 92.77(5)° is larger than the angle at S3 (Sn1–S3–Sn1a) with 87.23(5)°. The other S–Sn–S angles range from 110.03(5) to 113.60(5)°, indicating a distortion from ideal tetrahedral geometry. The {[Mn(tren)]$_2$Sn$_2$S$_6$} molecules are arranged in a chain-like manner along [010] (Fig. 5), and the [Mn(tren)]$^{2+}$ cations point alternatingly up and down along this direction. This arrangement results in a packing of the molecules in layers within the (100) plane which are stacked along [100] (Fig. 5). The terminal S atoms have relatively short contacts to N atoms in the range 2.576 – 2.934 Å (Fig. 6) indicating hydrogen bonding interactions.

We note that the compound is isostructural to {[Co(tren)]$_2$Sn$_2$S$_6$} [25] and the topology bears also similarity to the compounds [Mn(en)$_3$]$_2$Sn$_2$S$_6$ [26] and [Mn(dien)$_2$]$_2$Sn$_2$S$_6$ [27].

Raman spectroscopy

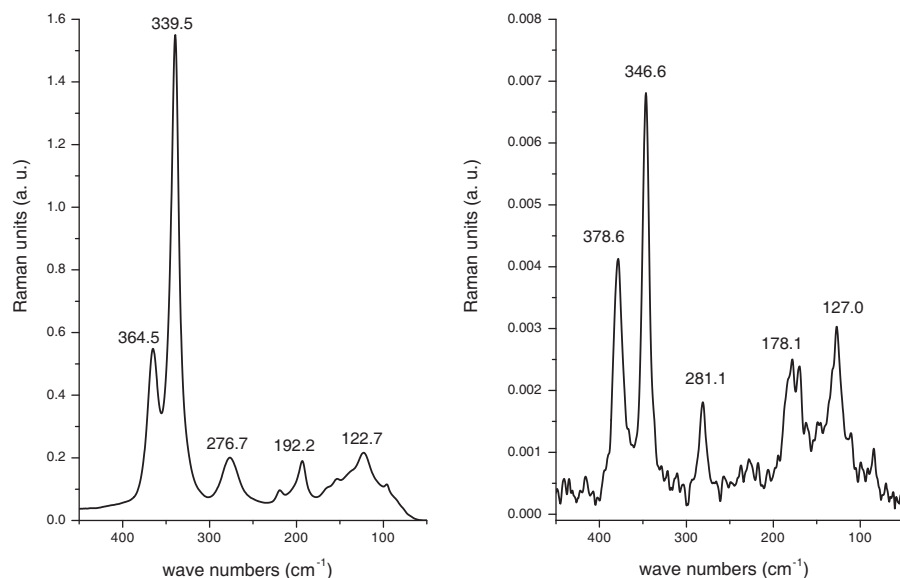The Raman spectra of both compounds are shown in Fig. 7.

Fig. 7. Comparison of the Raman spectra of (trenH)$_2$Sn$_3$S$_7$ (**1**) (left) and {[Mn(tren)]$_2$Sn$_2$S$_6$} (**2**) (right). The characteristic signals are labelled.

The three Sn–S stretching modes of the SnS$_5$ polyhedron of **1** are in the range $400 - 250$ cm^{-1} [59]. An asymmetric stretching vibration occurs at 364 cm^{-1} for **1** and at 378 cm^{-1} for **2**, and the symmetric stretching modes of the equatorial SnS$_3$ unit at 340 and 346 cm^{-1}, respectively. The signals at 278 and 281 cm^{-1} are assigned to the symmetric stretching vibration of the Sn$_2$S$_2$ ring [35, 60].

Conclusions

The layered compound (trenH)$_2$Sn$_3$S$_7$ (**1**) is a new members of the *R*-SnS-1 thiostannate family. The structure features the typical Sn$_3$S$_4$ semi-cubes which are constructed by edge-sharing SnS$_5$ trigonal bipyramids. The semi-cubes are joined *via* common edges yielding the anionic [Sn$_3$S$_7$]$^{2-}$ layers with pore sizes of about 11×11 Å^2. The protonated amine molecules act as charge compensating cations and structure-directing agents. It is most likely that they are located above and below the pores and between the layers.

Crystal structure determination of such layered compounds is often difficult because the thin platelet-like crystals are twisted and shifted against each other (see Fig. 3). One way to improve the crystal quality and to avoid the disorder of the crystallites are growth experiments without gravitational force as demonstrated in 1997 by Ozin and co-workers who obtained very good crystals of (TMA)$_2$Sn$_3$S$_7$ in a space lab [59].

The structure of **2** features the typical thiostannate anion [Sn$_2$S$_6$]$^{4-}$ connected to two [Mn(tren)]$^{2+}$ complexes *via* Mn–S bonds forming the neutral moiety {[Mn(tren)]$_2$Sn$_2$S$_6$} instead of discrete ions as could be found in many other thiostannate compounds.

In the Raman spectra of both compounds typical modes of the thiostannate anions are observed, and the different shifts are in agreement with the Sn–S bond lengths of the compounds.

[1] W. S. Sheldrick, M. Wachhold, *Coord. Chem. Rev.* **1998**, *176*, 211 – 322.
[2] W. S. Sheldrick, *J. Chem. Soc., Dalton Trans.* **2000**, 3041 – 3052.
[3] X. H. Bu, N. F. Zheng, P. Y. Feng, *Chem. Eur. J.* **2004**, *10*, 3356 – 3362.
[4] P. Y. Feng, X. H. Bu, N. F. Zheng, *Acc. Chem. Res.* **2005**, *38*, 293 – 303.

[5] S. Dehnen, M. Melullis, *Coord. Chem. Rev.* **2007**, *251*, 1259 – 1280.

[6] M. G. Kanatzidis, *Adv. Mater.* **2007**, *19*, 1165 – 1181.

[7] Q. C. Zhang, X. H. Bu, Z. Lin, T. Wu, P. Y. Feng, *Inorg. Chem.* **2008**, *47*, 9724 – 9726.

[8] J. Zhou, J. Dai, G. Q. Bian, C. Y. Li, *Coord. Chem. Rev.* **2009**, *253*, 1221 – 1247.

[9] R. L. Bedard, L. D. Vail, S. T. Wilson, E. M. Flanigen, U. S. Patent 4880761, **1989**.

[10] R. L. Bedard, L. D. Vail, S. T. Wilson, E. M. Flanigen, U. S. Patent 4933068, **1990**.

[11] R. L. Bedard, S. T. Wilson, L. D. Vail, J. M. Bennett, E. M. Flanigen, *Stud. Surf. Sci. Catal.* **1989**, *49*, 375 – 387.

[12] B. Seidlhofer, N. Pienack, W. Bensch, *Z. Naturforsch.* **2010**, *65b*, 937 – 975.

[13] M. Behrens, C. Näther, W. Bensch, *Z. Anorg. Allg. Chem.* **2002**, *628*, 2160 – 2160.

[14] C. Näther, S. Scherb, W. Bensch, *Acta Crystallogr.* **2003**, *E59*, m280–m282.

[15] A. Puls, C. Näther, W. Bensch, *Acta Crystallogr.* **2005**, *E61*, m868–m870.

[16] J. B. Parise, Y. H. Ko, J. Rijssenbeek, D. M. Nellis, K. M. Tan, S. Koch, *J. Chem. Soc., Chem. Commun.* **1994**, 527 – 527.

[17] S. Dehnen, C. Zimmermann, *Z. Anorg. Allg. Chem.* **2002**, *628*, 2463 – 2469.

[18] T. Jiang, A. Lough, G. A. Ozin, *Adv. Mater.* **1998**, *10*, 42 – 46.

[19] T. Jiang, A. Lough, G. A. Ozin, R. L. Bedard, R. Broach, *J. Mater. Chem.* **1998**, *8*, 721 – 732.

[20] R. J. Francis, S. J. Price, J. S. O. Evans, S. O'Brien, D. O'Hare, S. M. Clark, *Chem. Mater.* **1996**, *8*, 2102 – 2108.

[21] T. Jiang, G. A. Ozin, *J. Mater. Chem.* **1997**, *7*, 2213 – 2222.

[22] R. W. J. Scott, M. J. MacLachlan, G. A. Ozin, *Curr. Opin. Solid St. M.* **1999**, *4*, 113 – 121.

[23] A. K. Cheetham, G. Férey, T. Loiseau, *Angew. Chem. Int. Ed.* **1999**, *38*, 3268 – 3292.

[24] D. X. Jia, J. Dai, Q. Y. Zhu, Y. Zhang, X. M. Gu, *Polyhedron* **2004**, *23*, 937 – 942.

[25] M. Behrens, S. Scherb, C. Näther, W. Bensch, *Z. Anorg. Allg. Chem.* **2003**, *629*, 1367 – 1373.

[26] D. X. Jia, Y. Zhang, J. Dai, Q. Y. Zhu, X. M. Gu, *Z. Anorg. Allg. Chem.* **2004**, *630*, 313 – 318.

[27] M. L. Fu, G. C. Guo, B. Liu, A. Q. Wu, J. S. Huang, *Chin. J. Inorg. Chem.* **2005**, *21*, 25 – 29.

[28] N. Pienack, C. Näther, W. Bensch, *Solid State Sci.* **2007**, *9*, 100 – 107.

[29] N. Pienack, C. Näther, W. Bensch, *Eur. J. Inorg. Chem.* **2009**, 937 – 946.

[30] R.-C. Zhang, H.-G. Yao, S.-H. Ji, M.-C. Liu, M. Ji, Y.-L. An, *Chem. Commun.* **2010**, *46*, 4550 – 4552.

[31] M. Behrens, M. E. Ordolff, C. Näther, W. Bensch, K. D. Becker, C. Guillot-Deudon, A. Lafond, J. A. Cody, *Inorg. Chem.* **2010**, *49*, 8305 – 8309.

[32] M. H. BaiYin, L. Ye, Y. L. An, X. Liu, C. Y. Jia, G. L. Ning, *Bull. Chem. Soc. Jpn.* **2005**, *78*, 1283 – 1284.

[33] N. Pienack, W. Bensch, *Z. Anorg. Allg. Chem.* **2006**, *632*, 1733 – 1736.

[34] N. Pienack, K. Möller, C. Näther, W. Bensch, *Solid State Sci.* **2007**, *9*, 1110 – 1114.

[35] N. Pienack, C. Näther, W. Bensch, *Z. Naturforsch.* **2008**, *63b*, 1243 – 1251.

[36] N. Pienack, C. Näther, W. Bensch, *Eur. J. Inorg. Chem.* **2009**, 1575 – 1577.

[37] X.-M. Gu, J. Dai, D.-X. Jia, Y. Zhang, Q.-Y. Zhu, *Cryst. Growth Des.* **2005**, *5*, 1845 – 1848.

[38] Z. Wang, G. Xu, Y. Bi, C. Wang, *CrystEngComm* **2010**, *12*, 3703 – 3707.

[39] G.-N. Liu, G.-C. Guo, F. Chen, S.-P. Guo, X.-M. Jiang, C. Yang, M. S. Wang, M.-F. Wu, J.-S. Huang, *CrystEngComm* **2010**, *12*, 4035 – 4037.

[40] G. M. Sheldrick, SHELXS-97, Program for the Solution of Crystal Structures, University of Göttingen, Göttingen (Germany) **1997**. See also: G. M. Sheldrick, *Acta Crystallogr.* **1990**, *A46*, 467 – 473.

[41] G. M. Sheldrick, SHELXL-97, Program for the Refinement of Crystal Structures, University of Göttingen, Göttingen (Germany) **1997**. See also: G. M. Sheldrick, *Acta Crystallogr.* **2008**, *A64*, 112 – 122.

[42] A. L. Spek, PLATON, A Multipurpose Crystallographic Tool, Utrecht University, Utrecht (The Netherlands) **2005**. See also: A. L. Spek, *J. Appl. Crystallogr.* **2009**, *D65*, 148 – 155.

[43] K. M. Tan, Y. G. Ko, J. B. Parise, *Acta Crystallogr.* **1995**, *C51*, 398 – 401.

[44] T. Jiang, A. J. Lough, G. A. Ozin, D. Young, R. L. Bedard, *Chem. Mater.* **1995**, *7*, 245 – 248.

[45] T. Jiang, A. Lough, G. A. Ozin, R. L. Bedard, *J. Mater. Chem.* **1998**, *8*, 733 – 741.

[46] T. Jiang, G. A. Ozin, *J. Mater. Chem.* **1998**, *8*, 1099 – 1108.

[47] W. S. Sheldrick, B. Schaaf, *Z. Anorg. Allg. Chem.* **1994**, *620*, 1041 – 1045.

[48] Z. Rejai, H. Lühmann, C. Näther, R. K. Kremer, W. Bensch, *Inorg. Chem.* **2010**, *49*, 1651 – 1657.

[49] M. Schaefer, D. Kurowski, A. Pfitzner, C. Näther, W. Bensch, *Inorg. Chem.* **2006**, *45*, 3726 – 3731.

[50] A. Puls, C. Näther, W. Bensch, *Z. Anorg. Allg. Chem.* **2006**, *632*, 1239 – 1243.

[51] M. Schaefer, C. Näther, N. Lehnert, W. Bensch, *Inorg. Chem.* **2004**, *43*, 2914 – 2921.

[52] M. Schaefer, R. Stähler, W.-R. Kiebach, C. Näther, W. Bensch, *Z. Anorg. Allg. Chem.* **2004**, *630*, 1816 – 1822.

[53] L. Engelke, R. Stähler, M. Schur, C. Näther, W. Bensch, R. Pöttgen, M. H. Möller, *Z. Naturforsch.* **2004**, *59b*, 869 – 876.

[54] M. Schur, C. Näther, W. Bensch, *Z. Naturforsch.* **2001**, *56b*, 79 – 84.

[55] H. Lühmann, Z. Rejai, K. Möller, P. Leisner, M. E. Ordolff, C. Näther, W. Bensch, *Z. Anorg. Allg. Chem.* **2008**, *634*, 1687 – 1695.

[56] A. Kromm, W. S. Sheldrick, *Z. Anorg. Allg. Chem.* **2008**, *634*, 2948 – 2953.

[57] Z. Wang, H. Zhang, C. Wang, *Inorg. Chem.* **2009**, *48*, 8180 – 8185.

[58] N. Pienack, S. Lehmann, H. Lühmann, M. El-Madani, C. Näther, W. Bensch, *Z. Anorg. Allg. Chem.* **2008**, *634*, 2323 – 2329.

[59] O. Däg, H. Ahari, N. Coombs, T. Jiang, P. P. Aroca-Ouellette, S. Petrov, I. Sokolov, A. Verma, G. Vovk, D. Young, G. A. Ozin, C. Reber, Y. Pelletier, R. L. Bedard, *Adv. Mater.* **1997**, *9*, 1133 – 1149.

[60] B. Krebs, S. Pohl, W. Schiwy, *Angew. Chem., Int. Ed. Engl.* **1970**, *9*, 897 – 898.